

# Performance Analysis of SNR Threshold-Setting Strategies for Adaptive Modulation and Coding under Fading Channels

Miguel López-Benítez

*Department of Electrical Engineering and Electronics  
University of Liverpool, United Kingdom*

---

## Abstract

Adaptive Modulation and Coding (AMC) is a popular technique that dynamically adapts the employed Modulation and Coding Scheme (MCS) to the instantaneous channel quality, typically expressed in terms of the instantaneous Signal-to-Noise Ratio (SNR). The optimum MCS is selected based on a set of SNR thresholds, which define the range of SNR values on which each MCS is employed. The calculation of the SNR thresholds is a key aspect in the design and performance of AMC. This work performs a detailed and rigorous analysis of SNR threshold setting strategies for AMC, not only considering conventional methods commonly used in the literature but also proposing new methods to attain specific performance targets in terms of error rate, delay and spectral/energy efficiency. Closed-form expressions for these performance metrics are analytically derived under Rayleigh fading and employed to comparatively assess the performance of the considered solutions. The obtained results demonstrate that the proposed SNR threshold setting methods provide significant improvements in terms of error rate, delay and spectral/energy efficiency with respect to traditional methods.

*Keywords:* Adaptive modulation and coding, link adaptation, Rayleigh fading, LTE.

---

## 1. Introduction

Wireless communication systems typically feature several Modulation and Coding Schemes (MCS) in order to provide varying levels of resilience to transmission errors under different radio propagation conditions and consequently adapt the transmission data rate. Each MCS is characterised by a different trade-off  
5 between data rate and error protection, which is determined by the modulation type and order, and the amount of redundant information introduced by the channel coding scheme. The employed MCS is dynamically adapted to the instantaneous channel quality in order to optimise the system performance: MCS with little or no error protection are used when the channel quality is favourable, while MCS with extra error protection are selected under poor channel quality conditions. This technique, referred to as Adaptive  
10 Modulation and Coding (AMC), has been adopted by several wireless communication technologies, including cellular mobile communication systems such as EDGE [1], HSDPA [2] and LTE [3, 4], wireless local [5, 6, 7], personal [8, 9, 10] and broadband [11, 12] area networks (IEEE 802.11/15/16) as well as satellite communication networks [13, 14], to mention some examples.

The method employed to select the optimum MCS is a key aspect in the design and performance of  
15 AMC. Existing methods can broadly be classified into two categories. The first category includes methods that adapt the employed MCS to the real-time variations of a certain performance metric (e.g., short-term error rate or throughput) with the aim to achieve a predefined performance target (e.g., long-term error rate or throughput) [6, 15, 8, 9, 2]. The second category, where the focus of this work lies, embraces methods that adapt the employed MCS to the instantaneous value of a certain link quality metric, typically the

---

*Email address:* [M.Lopez-Benitez@liverpool.ac.uk](mailto:M.Lopez-Benitez@liverpool.ac.uk) (Miguel López-Benítez)

instantaneous Signal to Noise Ratio (SNR). The optimum MCS is selected by comparing the instantaneous SNR to a set of SNR thresholds that determine the range of SNR values where each MCS is employed. In this type of methods the criterion employed to compute the SNR thresholds has an important impact on the resulting AMC performance. A criterion commonly used in the literature is to select the SNR thresholds so as to maximise the throughput [16, 11, 12, 15, 2]. This criterion, however, may sometimes result in high error rates and therefore in a high number of retransmissions, thus leading to a degraded performance for delay-sensitive services. To avoid frequent retransmissions, a common alternative criterion is to maximise the throughput subject to a maximum target error rate [1, 11, 15, 17]. Other delay-oriented methods recompute the SNR thresholds for each transmitted packet based on the packet size and reception deadline in order to optimise the delay performance [18, 19, 15]. The maximisation of the user quality of experience (e.g., the image quality of video services [20]) has also been proposed. More recently, some investigations have included energy efficiency aspects into SNR threshold selection criteria [21, 22, 10].

While AMC has received a great deal of attention, the performance of SNR threshold-setting methods for AMC has not received to date a unified, formal and rigorous treatment where fundamental methods are analysed and compared under a common unified framework. Many theoretical results lack of sufficient practical applicability in the design and performance evaluation of real wireless communication systems. For instance, a commonly used approach for the analysis of AMC under fading channels is to employ the Shannon capacity [23], or a modified version thereof [24, 25], as a model for the transmission data rates. The expressions thus obtained are of theoretical value and can provide interesting insights but can hardly be employed to predict the actual performance of real systems since the particular features of individual MCS cannot be captured by such models. By contrast, some other studies have provided more detailed and realistic models. For example, throughput performance models are obtained analytically in [26] for AMC under log-normal shadow fading, in [27] for maximum ratio combining receivers with AMC under Rice fading correlated channels, and in [28] for a broader set of fading models including Rayleigh, Nakagami- $m$ , Nakagami- $q$  (Hoyt), Nakagami- $n$  (Rice),  $\eta$ - $\mu$  and  $\kappa$ - $\mu$ . However, the developed models have not been employed to comparatively evaluate the performance of existing SNR threshold-setting methods along with their merits and shortcomings. Moreover, as it will be shown, traditional methods commonly used to compute the SNR thresholds are in general unable to meet certain performance requirements, or are able to do so to a limited extent.

In this context, this work performs a detailed and rigorous performance analysis of SNR threshold-setting strategies for AMC. Based on a technology- and service-agnostic approach (i.e., without considering particular features of specific radio technologies or services, and abstracting them wherever required), this work reviews the fundamental methods for the calculation of SNR thresholds and proposes new strategies to effectively and more accurately achieve specific performance targets in terms of error rate, delay and spectral/energy efficiency. Moreover, closed-form expressions for these performance metrics are analytically derived and employed to comparatively assess the performance of existing and proposed SNR threshold-setting methods. The following contributions are provided by this work:

1. A generic model for the error performance of MCS under AWGN is proposed. As opposed to existing models, which have been envisaged for either analytical tractability or practical accuracy, the proposed model not only is analytically tractable but also reproduces with remarkable accuracy the actual error rate of MCS from real wireless communication systems.
2. Fundamental SNR threshold-setting methods commonly used in the existing literature are formulated analytically under a common technology- and service-agnostic unified framework.
3. Novel SNR threshold-setting methods envisaged to accurately meet specific performance targets in terms of error rate, delay and spectral/energy efficiency are proposed as well.
4. Closed-form expressions for the average error rate, delay and spectral/energy efficiency of SNR threshold-setting methods under fading channels are derived analytically.
5. The performance of the considered SNR threshold-setting strategies is assessed and comparatively evaluated under fading channels, highlighting their benefits, costs, advantages and drawbacks.

The rest of this work is organised as follows. First, Section 2 presents the considered system model. A generic model for the error performance of MCS under AWGN is proposed in Section 3. Based on

this model, closed-form expressions for the error rate, delay and spectral/energy efficiency are analytically derived in Section 4. Existing and new SNR threshold-setting methods are formulated in Sections 5 and 6. The performance of the considered methods is comparatively assessed in Section 7, where numerical results obtained with the developed analytical models are presented and analysed. A discussion on the extension to specific radio technologies is provided in Section 8. Finally, Section 9 summarises and concludes this work.

## 2. System Model

Let  $N$  denote the number of MCS available in the considered wireless communication system. Each MCS can be characterised by two properties:  $\varepsilon_n(\gamma)$ , which represents the error rate at the bit (BER), symbol (SER), block (BLER), packet (PER) or frame (FER) level of the  $n$ th MCS as a function of the instantaneous SNR  $\gamma$ ; and  $R_n$ , which represents the gross data rate of the  $n$ th MCS (i.e., the total amount of information bits transmitted per time unit). MCS are indexed such that  $R_n < R_{n+1}$ ,  $n = 1, \dots, N - 1$ .

The employed MCS is dynamically adapted to the instantaneous SNR based on a set of SNR thresholds  $\{\gamma_n^{th}\}_{n=1}^N$ , which define the range of values of  $\gamma$  on which each MCS is used. The  $n$ th MCS is selected whenever  $\gamma \in [\gamma_n^{th}, \gamma_{n+1}^{th})$ , except for the  $N$ th MCS which is used in the interval  $\gamma \in [\gamma_N^{th}, \infty)$ .

An SNR threshold-setting method is defined as a method to compute the values  $\{\gamma_n^{th}\}_{n=1}^N$  based on  $\varepsilon_n(\gamma)$ ,  $R_n$ , and possibly other parameters, according to a predefined criterion. Two types of methods are distinguished in this work: *unconstrained* methods ( $\gamma_1^{th} = 0$ ) which always select an MCS for the current SNR value no matter how low it is, and *constrained* methods ( $\gamma_1^{th} > 0$ ) which allow transmission only when the instantaneous SNR is above a *cut-off* threshold  $\gamma_1^{th}$ . The latter approach prevents the transmission of users under extremely poor channel quality conditions (who might not benefit from transmitting) so that other users in better conditions can exploit the available radio resources more efficiently.

## 3. Model for the Error Performance of MCS

The bit and symbol error probabilities of modulation schemes under AWGN are well known from the theory of digital communication systems. The error probabilities for groups of bits such as blocks, packets or frames, which quantify more accurately the actual performance experienced by the user at higher layers, can be approximated by the probability of receiving at least one bit in error [29]. However, the introduction of channel coding techniques to increase the robustness against transmission errors complicates the analytical derivation of closed-form expressions for the error probabilities of MCS. As a result, a common approach is to fit a mathematical model to the exact curves  $\varepsilon_n(\gamma)$ , which are typically obtained by means of simulations.

Some proposed approximations can be easily manipulated in analytical studies but fail to provide a practical level of accuracy over the whole range of SNR values [30, eq. (3)], [31, eq. (5)]. Other approximations are accurate but difficult to manipulate in analytical studies [32, eq. (5)]. To overcome this drawback, the following model is here proposed:

$$\varepsilon_n(\gamma) = \mathcal{Q}(\alpha_n \gamma - \beta_n) \quad (1)$$

where  $\mathcal{Q}(x) = \frac{1}{\sqrt{2\pi}} \int_x^\infty \exp(-z^2/2) dz$  is the Gaussian Q-function and  $\alpha_n > 0$  and  $\beta_n > 0$  are MCS-specific fitting coefficients. As a part of this work, the model in (1) was fitted to the BLER-versus-SNR curves<sup>1</sup> of the LTE system provided in [33, Fig. 5] and a maximum absolute error of less than 1% was observed. Thus, the proposed model not only provides the desired analytical tractability but also sufficient accuracy.

## 4. Performance Metrics

Based on the model in (1), this section derives closed-form expressions for relevant performance metrics under Rayleigh fading channels, i.e., assuming an SNR probability density function given by  $f_\gamma(\gamma) = (1/\bar{\gamma}) \exp(-\gamma/\bar{\gamma})$  where  $\bar{\gamma}$  is the average SNR. The analytical results here obtained will be useful not only for performance evaluation purposes but also for the development of new SNR threshold-setting methods.

<sup>1</sup>The expression in (1) may also be fitted to similar curves available in the literature for other error metrics such as BER, SER, PER, FER, etc.

#### 4.1. Probability of Transmission

The probability of transmission is the probability that a user transmits (i.e., the complementary probability of outage), which is equivalent to the probability that the instantaneous SNR is above the *cut-off* SNR threshold. Under Rayleigh fading this metric is given by:

$$p_{tx}(\bar{\gamma}) = P(\gamma > \gamma_1^{th}) = \int_{\gamma_1^{th}}^{\infty} f_{\gamma}(\gamma) d\gamma = \exp\left(-\frac{\gamma_1^{th}}{\bar{\gamma}}\right) \quad (2)$$

Notice that  $p_{tx}(\bar{\gamma}) = 1$  for unconstrained methods and  $p_{tx}(\bar{\gamma}) < 1$  for constrained methods.

#### 4.2. Average Error Rate

The average error rate represents the average probability that a *data unit* (i.e., block, packet, frame, etc.) is received in error. For a particular set of SNR thresholds, this metric can be obtained by averaging  $\varepsilon_n(\gamma)$  for all MCS over the SNR statistics, taking into account the corresponding SNR range on which each MCS is used. The result can be expressed as:

$$\bar{\varepsilon}(\bar{\gamma}) = \frac{1}{p_{tx}(\bar{\gamma})} \left[ \sum_{n=1}^{N-1} \bar{\varepsilon}_n(\bar{\gamma}) + \bar{\varepsilon}_N(\bar{\gamma}) \right] \quad (3)$$

where  $\bar{\varepsilon}_n(\bar{\gamma})$  and  $\bar{\varepsilon}_N(\bar{\gamma})$  are given by (4) and (5) respectively:

$$\begin{aligned} \bar{\varepsilon}_n(\bar{\gamma}) = \int_{\gamma_n^{th}}^{\gamma_{n+1}^{th}} \varepsilon_n(\gamma) f_{\gamma}(\gamma) d\gamma &= \exp\left(-\frac{\gamma_n^{th}}{\bar{\gamma}}\right) \varepsilon_n(\gamma_n^{th}) - \exp\left(-\frac{\gamma_{n+1}^{th}}{\bar{\gamma}}\right) \varepsilon_n(\gamma_{n+1}^{th}) \\ &\quad - \exp\left(\frac{1 - 2\alpha_n \beta_n \bar{\gamma}}{2\alpha_n^2 \bar{\gamma}^2}\right) \left[ \varepsilon_n\left(\gamma_n^{th} + \frac{1}{\alpha_n^2 \bar{\gamma}}\right) - \varepsilon_n\left(\gamma_{n+1}^{th} + \frac{1}{\alpha_n^2 \bar{\gamma}}\right) \right] \end{aligned} \quad (4)$$

$$\bar{\varepsilon}_N(\bar{\gamma}) = \int_{\gamma_N^{th}}^{\infty} \varepsilon_N(\gamma) f_{\gamma}(\gamma) d\gamma = \exp\left(-\frac{\gamma_N^{th}}{\bar{\gamma}}\right) \varepsilon_N(\gamma_N^{th}) - \exp\left(\frac{1 - 2\alpha_N \beta_N \bar{\gamma}}{2\alpha_N^2 \bar{\gamma}^2}\right) \varepsilon_N\left(\gamma_N^{th} + \frac{1}{\alpha_N^2 \bar{\gamma}}\right) \quad (5)$$

The expression for  $\bar{\varepsilon}_n(\bar{\gamma})$  is obtained by using the equality  $\mathcal{Q}(x) = \frac{1}{2}[1 - \text{erf}(x/\sqrt{2})]$ , where  $\text{erf}(x) = \frac{2}{\sqrt{\pi}} \int_0^x \exp(-z^2) dz$  is the Gaussian error function, and rearranging the integral in terms of the error function. The obtained result can be expressed in a compact form as shown in (4). This expression can be simplified since in general  $\varepsilon_n(\gamma_{n+1}^{th} + \phi) \approx 0$  ( $\phi \geq 0$ )<sup>2</sup>. The expression in (5) is obtained as  $\bar{\varepsilon}_N(\bar{\gamma}) = \lim_{\gamma_{n+1}^{th} \rightarrow \infty} \bar{\varepsilon}_n(\bar{\gamma})|_{n=N}$ .

Notice that a normalisation factor  $p_{tx}(\bar{\gamma})$  is required in (3) in order to provide the correct value for constrained methods. In constrained methods the error probabilities of individual MCS,  $\varepsilon_n(\gamma)$ , are not integrated over the whole range of values of the SNR statistics, i.e.,  $\gamma \in [0, \infty)$ , but only in the interval  $\gamma \in [\gamma_1^{th}, \infty)$ , which leads to an underestimation of the average error rate. The required normalisation factor is obtained by noting that  $\bar{\varepsilon}(\bar{\gamma}) = 1$  should be true when  $\varepsilon_n(\gamma) = 1$  for all MCS, regardless of  $\gamma_1^{th}$ . In such a case the sum of the integrals in (4)–(5) yields:

$$\sum_{n=1}^{N-1} \int_{\gamma_n^{th}}^{\gamma_{n+1}^{th}} 1 \cdot f_{\gamma}(\gamma) d\gamma + \int_{\gamma_N^{th}}^{\infty} 1 \cdot f_{\gamma}(\gamma) d\gamma = \int_{\gamma_1^{th}}^{\infty} f_{\gamma}(\gamma) d\gamma = \exp\left(-\frac{\gamma_1^{th}}{\bar{\gamma}}\right) = p_{tx}(\bar{\gamma}) \quad (6)$$

which is less than one for constrained methods ( $\gamma_1^{th} > 0$ ). Hence, the sum of the integrals in (4)–(5) needs to be normalised by (6), thus leading to (3).

<sup>2</sup>As shown in Fig. 1,  $\varepsilon_n(\gamma)$  rapidly decreases with  $\gamma$ . Thus, an appreciable increase/decrease of  $\gamma$  above/below the intended  $\gamma_n^{th}$  rapidly makes  $\varepsilon_n(\gamma)$  approach the values 0/1. This approximation was observed to be valid in most practical cases.

### 4.3. Average Throughput

The average throughput or net data rate represents the average number of information bits correctly delivered per time unit. The throughput of an individual MCS can be expressed as  $\Gamma_n(\gamma) = R_n[1 - \varepsilon_n(\gamma)]$ . Hence, the average throughput can be obtained by averaging  $\Gamma_n(\gamma)$  for all MCS over the SNR statistics, taking into account the corresponding SNR range on which each MCS is used. The result can be expressed as:

$$\bar{\Gamma}(\bar{\gamma}) = \sum_{n=1}^{N-1} \bar{\Gamma}_n(\bar{\gamma}) + \bar{\Gamma}_N(\bar{\gamma}) \quad (7)$$

where

$$\bar{\Gamma}_n(\bar{\gamma}) = \int_{\gamma_n^{th}}^{\gamma_{n+1}^{th}} \Gamma_n(\gamma) f_\gamma(\gamma) d\gamma = R_n \left[ \exp\left(-\frac{\gamma_n^{th}}{\bar{\gamma}}\right) - \exp\left(-\frac{\gamma_{n+1}^{th}}{\bar{\gamma}}\right) - \bar{\varepsilon}_n(\bar{\gamma}) \right] \quad (8)$$

$$\bar{\Gamma}_N(\bar{\gamma}) = \int_{\gamma_N^{th}}^{\infty} \Gamma_N(\gamma) f_\gamma(\gamma) d\gamma = R_N \left[ \exp\left(-\frac{\gamma_N^{th}}{\bar{\gamma}}\right) - \bar{\varepsilon}_N(\bar{\gamma}) \right] \quad (9)$$

The expression in (7) represents the average *effective* throughput, which takes into account both periods of activity ( $\gamma \geq \gamma_1^{th}$ ) and inactivity ( $\gamma < \gamma_1^{th}$ ) of the transmitter (i.e., the number of information bits correctly delivered divided by the time period elapsed between the first and last transmissions, including periods of inactivity). An average *active* throughput could be defined as  $\bar{\Gamma}(\bar{\gamma})/p_{tx}(\bar{\gamma})$ , which represents the throughput experienced while the transmitter is active (i.e., ignoring periods of inactivity). Both metrics are equivalent for unconstrained methods but their values differ for constrained methods (*active* throughput is greater than *effective* throughput). The *effective* throughput as defined in (7) represents more accurately the actual data rate performance experienced by the user and is therefore considered in this work as the throughput metric.

### 4.4. Average Normalised Delay

The average normalised delay is defined in this work as the average number of slots (or equivalent transmission intervals for the particular system under consideration) employed to transmit a volume of data that under ideal conditions (i.e., using the highest MCS with no transmission errors nor restrictions) would require one single slot for correct reception. Note that under ideal conditions the highest MCS can transmit a packet of  $R_N$  information bits in one time unit. Transmitting the same amount of data using the  $n$ th MCS with an actual data rate of  $R_n[1 - \varepsilon_n(\gamma)]$  bits per time unit would require  $\tau_n(\gamma) = R_N/(R_n[1 - \varepsilon_n(\gamma)])$  time units, which represents the normalised delay of the  $n$ th MCS. The average normalised delay could be calculated by averaging  $\tau_n(\gamma)$  for all MCS over the SNR statistics, taking into account the corresponding SNR range on which each MCS is used. This approach, however, leads to an integral that cannot be solved in closed-form without resorting to approximations. As a result, an alternative approach is considered in this section to obtain an expression for the average normalised delay, which not only leads to similar numerical results but also provides interesting insights that will be exploited in Section 6.4 to develop a novel threshold-setting method.

Let  $\bar{\nu}(\bar{\gamma})$  denote the average number of transmissions of a data unit (e.g., a packet), including the first transmission and subsequent retransmissions until it is correctly received. A packet will require  $k$  transmissions when each of the  $k - 1$  first transmissions is unsuccessful, which can occur with probability  $\bar{\varepsilon}(\bar{\gamma})$ , and the next transmission is successful, which can occur with probability  $1 - \bar{\varepsilon}(\bar{\gamma})$ . Therefore the probability of requiring  $k$  transmissions for correct reception is given by  $p_k(\bar{\gamma}) = [\bar{\varepsilon}(\bar{\gamma})]^{k-1} [1 - \bar{\varepsilon}(\bar{\gamma})]$  and the average number of transmissions can be computed as (see the appendix):

$$\bar{\nu}(\bar{\gamma}) = \sum_{k=1}^{\infty} p_k(\bar{\gamma}) k = [1 - \bar{\varepsilon}(\bar{\gamma})] \sum_{k=1}^{\infty} k [\bar{\varepsilon}(\bar{\gamma})]^{k-1} = \frac{1}{1 - \bar{\varepsilon}(\bar{\gamma})} \quad (10)$$

A user with transmission restrictions (i.e.,  $\gamma_1^{th} > 0$ ) will transmit in a fraction  $p_{tx}(\bar{\gamma}) < 1$  of the slots. Therefore, the number of slots required to perform the  $\bar{\nu}(\bar{\gamma})$  transmissions required by a data packet is given

by  $\bar{\nu}(\bar{\gamma})/p_{tx}(\bar{\gamma})$ . Notice that the highest MCS can transmit a packet of  $R_N$  information bits in one time unit. However, if the average *active* gross data rate  $\bar{R}(\bar{\gamma})$  is lower than  $R_N$ , transmitting the same amount of data would require  $R_N/\bar{R}(\bar{\gamma})$  packets. Each of these packets will require  $\bar{\nu}(\bar{\gamma})$  transmissions, which will take place in  $\bar{\nu}(\bar{\gamma})/p_{tx}(\bar{\gamma})$  slots. Thus, the average normalised delay as defined in this work is given by:

$$\tau(\bar{\gamma}) = \frac{R_N}{\bar{R}(\bar{\gamma})} \frac{\bar{\nu}(\bar{\gamma})}{p_{tx}(\bar{\gamma})} = \frac{R_N}{p_{tx}(\bar{\gamma}) \bar{R}(\bar{\gamma}) [1 - \bar{\varepsilon}(\bar{\gamma})]} \quad (11)$$

where  $\bar{R}(\bar{\gamma})$  is the average *active* gross data rate:

$$\bar{R}(\bar{\gamma}) = \frac{1}{p_{tx}(\bar{\gamma})} \left[ \sum_{n=1}^{N-1} \bar{R}_n(\bar{\gamma}) + \bar{R}_N(\bar{\gamma}) \right] \quad (12)$$

and

$$\bar{R}_n(\bar{\gamma}) = \int_{\gamma_n^{th}}^{\gamma_{n+1}^{th}} R_n f_\gamma(\gamma) d\gamma = R_n \left[ \exp\left(-\frac{\gamma_n^{th}}{\bar{\gamma}}\right) - \exp\left(-\frac{\gamma_{n+1}^{th}}{\bar{\gamma}}\right) \right] \quad (13)$$

$$\bar{R}_N(\bar{\gamma}) = \int_{\gamma_N^{th}}^{\infty} R_N f_\gamma(\gamma) d\gamma = R_N \exp\left(-\frac{\gamma_N^{th}}{\bar{\gamma}}\right) \quad (14)$$

The metric  $\tau(\bar{\gamma})$  represents the average number of slots required for the correct reception of a certain volume of data that under ideal conditions would require one single slot. It can readily be shown that  $\tau(\bar{\gamma}) \in [1, \infty)$ . Concretely,  $\lim_{\bar{\gamma} \rightarrow 0} \tau(\bar{\gamma}) = \infty$  (low SNR conditions) and  $\lim_{\bar{\gamma} \rightarrow \infty} \tau(\bar{\gamma}) = 1$  (high SNR conditions), the latter corresponding to the ideal case  $\bar{R}(\bar{\gamma}) = R_N$  (use of the highest MCS),  $p_{tx}(\bar{\gamma}) = 1$  (no restrictions) and  $\bar{\varepsilon}(\bar{\gamma}) = 0$  (no errors).

The result in (11) includes the effect of the gross data rate of the selected MCS (higher data rate implies lower number of transmissions for a given volume of data), their error probabilities (more errors implies more retransmissions) and the transmission constraints (lower probability of transmission also implies higher delay). The actual transmission delay would also be affected by other additional factors (e.g., resource scheduling algorithms), however the definition considered in this work is aimed at capturing exclusively the individual impact of AMC.

#### 4.5. Average Normalised Energy Consumption

While different MCS yield different energy consumption levels in digital circuits, the difference is negligible compared to the energy consumption of analogical and radio frequency front-end circuits [34]. Therefore, the energy consumption is predominantly determined by the total time that a transmitter needs to be active in order to successfully transmit a certain amount of data. Based on this observation, the average energy consumption of an SNR threshold-setting method can be quantified by means of (11), taking into account that energy is consumed only when the transmitter is active, thus leading to the following definition:

$$\eta(\bar{\gamma}) = \frac{R_N}{\bar{R}(\bar{\gamma})} \bar{\nu}(\bar{\gamma}) = \frac{R_N}{\bar{R}(\bar{\gamma}) [1 - \bar{\varepsilon}(\bar{\gamma})]} \quad (15)$$

which represents the average number of slots that a transmitter needs to be active in order to successfully transmit a volume of data that under ideal conditions (i.e., use of the highest MCS and no transmission errors) would require one single active slot.

## 5. Unconstrained Threshold-Setting Strategies

This section presents unconstrained SNR threshold-setting strategies for AMC, where  $\gamma_1^{th} = 0$  and the rest of SNR thresholds are computed based on a certain criterion.

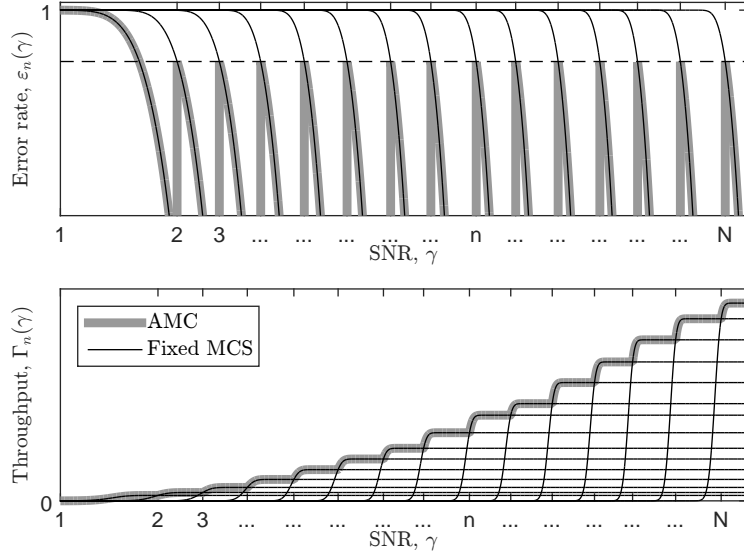


Figure 1: Instantaneous error (top) and throughput (bottom) performances of fixed MCS and AMC versus instantaneous SNR.

### 5.1. Unconstrained Maximum Throughput Strategy (U-MTS)

A criterion commonly used in the existing literature is to maximise the throughput (i.e., the net data rate) by selecting the MCS that provides the highest throughput for the current instantaneous SNR (see Fig. 1). The throughput of an individual MCS is given by  $\Gamma_n(\gamma) = R_n[1 - \varepsilon_n(\gamma)]$ . As shown in Fig. 1, the SNR threshold  $\gamma_n^{th}$  for the  $n$ th MCS is the SNR value where its throughput is equal to that of the  $(n-1)$ th MCS. Thus, the  $n$ th SNR threshold can be obtained by solving the equation  $\Gamma_n(\gamma_n^{th}) = \Gamma_{n-1}(\gamma_n^{th})$ , or  $R_n[1 - \varepsilon_n(\gamma_n^{th})] = R_{n-1}[1 - \varepsilon_{n-1}(\gamma_n^{th})]$ . Using the approximation  $\varepsilon_{n-1}(\gamma_n^{th}) \approx 0$ , which is acceptable as shown in Fig. 1, yields:

$$\gamma_n^{th} = \begin{cases} 0 & n = 1 \\ \varepsilon_n^{-1} \left( 1 - \frac{R_{n-1}}{R_n} \right) = \frac{1}{\alpha_n} \left[ \beta_n + \mathcal{Q}^{-1} \left( 1 - \frac{R_{n-1}}{R_n} \right) \right] & n = 2, \dots, N \end{cases} \quad (16a)$$

$$(16b)$$

### 5.2. Unconstrained Maximum Error Strategy (U-MES)

To avoid frequent retransmissions, a common alternative criterion is to maximise the throughput subject to a maximum target error rate  $\varepsilon_{max}$ , which can be achieved by selecting the MCS, out of all the MCS satisfying the condition  $\varepsilon_n(\gamma) \leq \varepsilon_{max}$ , that provides the highest throughput (see Fig. 1). Since  $\varepsilon_n(\gamma)$  is a decreasing function of  $\gamma$ , the SNR threshold for the  $n$ th MCS can be obtained as the SNR value where  $\varepsilon_n(\gamma) = \varepsilon_{max}$ , which yields:

$$\gamma_n^{th} = \begin{cases} 0 & n = 1 \\ \varepsilon_n^{-1}(\varepsilon_{max}) = \frac{1}{\alpha_n} \left[ \beta_n + \mathcal{Q}^{-1}(\varepsilon_{max}) \right] & n = 2, \dots, N \end{cases} \quad (17a)$$

$$(17b)$$

### 5.3. Unconstrained Minimum Delay and Minimum Energy Consumption Strategies

The aim of the minimum-delay strategy is to minimise the delay by selecting the MCS that provides the lowest normalised delay, which can be defined (see Section 4.4) as  $\tau_n(\gamma) = R_n / (R_n[1 - \varepsilon_n(\gamma)])$ . With this method, the SNR threshold  $\gamma_n^{th}$  for the  $n$ th MCS is the SNR value where its normalised delay is equal to that of the  $(n-1)$ th MCS. Thus,  $\gamma_n^{th}$  can be computed by solving the equation  $\tau_n(\gamma_n^{th}) = \tau_{n-1}(\gamma_n^{th})$ , which leads to the equation  $\Gamma_n(\gamma_n^{th}) = \Gamma_{n-1}(\gamma_n^{th})$  and therefore to the same SNR thresholds obtained in (16) for the

U-MTS method. Based on the same reasoning of Section 4.5, the energy consumption for an individual MCS is proportional to  $R_N/(R_n[1 - \varepsilon_n(\gamma)])$ . Therefore, the strategies of maximising the throughput, minimising the delay and minimising the energy consumption lead to the same set of SNR thresholds for AMC.

Note that the definition of delay (Section 4.4) and the resulting definition of energy consumption (Section 4.5) considered in this work are aimed at exclusively capturing the individual impact of AMC. Under such consideration, the strategies of optimising throughput, delay and energy consumption are equivalent (i.e., they lead to the same set of SNR thresholds). These performance metrics may actually depend on other additional factors not directly related with AMC, which as a result might lead to different sets of SNR thresholds when taken into account, however such factors are out of the scope of this work.

## 6. Constrained Threshold-Setting Strategies

When the instantaneous channel quality degrades, the probability of suffering transmission errors increases and the experienced throughput, delay and energy consumption performances can therefore be expected to degrade. During periods of sufficiently poor channel quality conditions the user may not obtain any benefit from transmitting (i.e., the transmitted bits would be received in error, which would not increase the throughput neither reduce the transmission delay, and would waste energy). During such periods, another user in better conditions could be allocated the channel without resulting in a noticeable performance degradation for the user under bad channel quality conditions. Although this problem is usually managed at the system level (e.g., by means of scheduling algorithms), it can also be addressed at the link level, which motivates the design of constrained SNR threshold-setting methods for AMC. This section formulates the constrained version ( $\gamma_1^{th} > 0$ ) of the methods presented in Section 5 and introduces new strategies designed to achieve specific performance targets.

### 6.1. Constrained Maximum Throughput Strategy (C-MTS)

It can be shown that any constrained version of the MTS method results in a lower average user throughput than the U-MTS method. The objective of the C-MTS method is to compute  $\gamma_1^{th} > 0$  so that the throughput performance degradation with respect to U-MTS can be considered negligible in practice. A constrained version of the MTS method, referred to as *mode 0*, was proposed in [16] and evaluated in [35]. The proposal of [16] adopts a system level approach where the channel quality variation caused by retransmissions is included in the threshold calculation. This work proposes simpler link level approaches for C-MTS.

The first proposed strategy, referred to as C-MTS-I, computes the SNR thresholds  $\{\gamma_n^{th}\}_{n=2}^N$  based on U-MTS and sets  $\gamma_1^{th}$  at the SNR value where the throughput of the first MCS,  $\Gamma_1(\gamma)$ , is a fraction  $\xi \in (0, 1)$  of its maximum achievable value. Hence,  $\gamma_1^{th}$  is obtained by solving the equation  $\Gamma_1(\gamma_1^{th}) = \xi \lim_{\gamma \rightarrow \infty} \Gamma_1(\gamma)$ , or  $R_1[1 - \varepsilon_1(\gamma_1^{th})] = \xi R_1$ , which yields:

$$\gamma_n^{th} = \begin{cases} \varepsilon_n^{-1}(1 - \xi) = \frac{1}{\alpha_n} [\beta_n + \mathcal{Q}^{-1}(1 - \xi)] & n = 1 & (18a) \\ \varepsilon_n^{-1} \left(1 - \frac{R_{n-1}}{R_n}\right) = \frac{1}{\alpha_n} \left[\beta_n + \mathcal{Q}^{-1} \left(1 - \frac{R_{n-1}}{R_n}\right)\right] & n = 2, \dots, N & (18b) \end{cases}$$

The second proposed strategy, referred to as C-MTS-II, is aimed at reducing the level of channel usage under low SNR conditions by forcing a certain probability of transmission  $\rho \in (0, 1)$ . Notice that if  $\rho < 1$  the level of usage of the channel will decrease, thus preventing the user from transmitting when the worst channel quality is experienced. The condition  $p_{tx}(\bar{\gamma}) = \rho$  yields the *cut-off* SNR threshold  $\gamma_{th} = \bar{\gamma} \ln(1/\rho)$ . Since  $\gamma_{th}$  is set regardless of the actual throughput performance and the rest of SNR thresholds, this may result in  $\gamma_{th}$  being greater than several of the SNR thresholds obtained with (16b)/(18b). Hence, the SNR thresholds for the C-MTS-II method are computed as:

$$\gamma_n^{th} = \max \left\{ \bar{\gamma} \ln \frac{1}{\rho}, \frac{1}{\alpha_n} \left[ \beta_n + \mathcal{Q}^{-1} \left( 1 - \frac{R_{n-1}}{R_n} \right) \right] \right\}, \quad n = 1, \dots, N \quad (19)$$



When several MCS share the same SNR threshold (this method may restrict the use of more than one MCS), only the highest one is used. Notice that the C-MTS-II *cut-off* threshold, in contrast with C-MTS-I, depends on the average channel quality, represented by  $\bar{\gamma}$ .

## 255 6.2. Constrained Maximum Error Strategy (C-MES)

The objective of the MES method is to maximise the throughput subject to a maximum target error rate  $\varepsilon_{max}$ . Notice that the error rate of the lowest MCS may exceed  $\varepsilon_{max}$  under poor channel quality conditions (see Fig. 1). This motivates a constrained version of the MES method where the limit on the maximum error probability is imposed on all MCS, including  $n = 1$ . Applying (17b) to all MCS yields:

$$\gamma_n^{th} = \varepsilon_n^{-1}(\varepsilon_{max}) = \frac{1}{\alpha_n} [\beta_n + \mathcal{Q}^{-1}(\varepsilon_{max})], \quad n = 1, \dots, N \quad (20)$$

## 260 6.3. Constrained Average Error Strategy (C-AES)

While the C-MES method guarantees that the desired maximum error rate  $\varepsilon_{max}$  is not exceeded, it cannot control the resulting average error rate  $\bar{\varepsilon}(\bar{\gamma})$ . The objective of the C-AES strategy is to compute the SNR thresholds so as to meet a predefined average error rate  $\varepsilon_{avg}$ .

Let  $\bar{\varepsilon}_{C-MES}(\bar{\gamma})$  denote the average error rate obtained with C-MES when  $\varepsilon_{max}$  is set equal to the desired target (i.e.,  $\varepsilon_{max} = \varepsilon_{avg}$ ). The error rate obtained this way, which satisfies  $\bar{\varepsilon}_{C-MES}(\bar{\gamma}) < \varepsilon_{avg}$ , needs to be increased in order to reach the target value  $\varepsilon_{avg}$ . Since the error rate  $\varepsilon_n(\gamma)$  is higher for low SNR values, this can be accomplished by decreasing the C-MES SNR thresholds. Several strategies are proposed to this end.

The first proposed strategy, referred to as C-AES-I, computes the SNR thresholds based on C-MES and then recomputes a lower  $\gamma_1^{th}$  so that the new threshold leads to a higher average error rate that meets the desired target (i.e.,  $\varepsilon_{avg}$  is obtained by decreasing  $\gamma_1^{th}$  while leaving the rest of SNR thresholds unchanged):

$$\gamma_n^{th} = \begin{cases} \lambda \gamma_{n,C-MES}^{th} & n = 1 \\ \gamma_{n,C-MES}^{th} & n = 2, \dots, N \end{cases} \quad (21a)$$

$$(21b)$$

where  $\gamma_{n,C-MES}^{th}$  denotes the C-MES SNR thresholds when  $\varepsilon_{max} = \varepsilon_{avg}$  and  $\lambda \in [0, 1)$  is the required reduction factor for  $\gamma_{1,C-MES}^{th}$ . The value of  $\lambda$  can be obtained by solving the equation resulting from reformulating (3) for a certain new SNR threshold  $\zeta_1 \gamma_{1,C-MES}^{th}$  and forcing the desired  $\varepsilon_{avg}$ :

$$\begin{aligned} \bar{\varepsilon}(\bar{\gamma}) &= \frac{1}{\exp\left(-\frac{-\zeta_1 \gamma_{1,C-MES}^{th}}{\bar{\gamma}}\right)} \left[ \int_{\zeta_1 \gamma_{1,C-MES}^{th}}^{\gamma_{1,C-MES}^{th}} \varepsilon_1(\gamma) f_\gamma(\gamma) d\gamma + \sum_{n=1}^{N-1} \bar{\varepsilon}_{n,C-MES}(\bar{\gamma}) + \bar{\varepsilon}_{N,C-MES}(\bar{\gamma}) \right] \\ &= \frac{\int_{\zeta_1 \gamma_{1,C-MES}^{th}}^{\gamma_{1,C-MES}^{th}} \varepsilon_1(\gamma) f_\gamma(\gamma) d\gamma}{\exp\left(-\frac{-\zeta_1 \gamma_{1,C-MES}^{th}}{\bar{\gamma}}\right)} + \frac{\exp\left(-\frac{-\gamma_{1,C-MES}^{th}}{\bar{\gamma}}\right)}{\exp\left(-\frac{-\zeta_1 \gamma_{1,C-MES}^{th}}{\bar{\gamma}}\right)} \bar{\varepsilon}_{C-MES}(\bar{\gamma}) = \varepsilon_{avg} \end{aligned} \quad (22)$$

where  $\zeta_1 \in [0, 1)$  represents a reduction factor for  $\gamma_{1,C-MES}^{th}$ . The solution to the integral in (22) can be readily obtained employing (4). However, the resulting expression cannot be solved analytically for  $\zeta_1$ . By choosing the value  $\zeta_1 = 1/2$  (i.e., the middle point of its numerical range), the problematic terms can be approximated by  $\varepsilon_1(\zeta_1 \gamma_{1,C-MES}^{th}) \approx \varepsilon_1(\frac{1}{2} \gamma_{1,C-MES}^{th}) \approx 1$  and  $\varepsilon_1(\zeta_1 \gamma_{1,C-MES}^{th} + 1/\alpha_1^2 \bar{\gamma}) \approx \varepsilon_1(\frac{1}{2} \gamma_{1,C-MES}^{th} + 1/\alpha_1^2 \bar{\gamma}) \approx 1$  since a reduction of the argument of  $\varepsilon_n(\cdot)$  rapidly increases its value towards one. Noting that  $\varepsilon_1(\gamma_{1,C-MES}^{th}) = \varepsilon_{max} = \varepsilon_{avg}$  yields:

$$\begin{aligned} \zeta_1 \approx & -\frac{\bar{\gamma}}{\gamma_{1,C-MES}^{th}} \ln \left\{ \frac{1}{1 - \varepsilon_{avg}} \left( \exp\left(-\frac{\gamma_{1,C-MES}^{th}}{\bar{\gamma}}\right) (\varepsilon_{avg} - \bar{\varepsilon}_{C-MES}(\bar{\gamma})) \right. \right. \\ & \left. \left. + \exp\left(\frac{1 - 2\alpha_1 \beta_1 \bar{\gamma}}{2\alpha_1^2 \bar{\gamma}^2}\right) \left[ 1 - \varepsilon_1\left(\gamma_{1,C-MES}^{th} + \frac{1}{\alpha_1^2 \bar{\gamma}}\right) \right] \right) \right\} \end{aligned} \quad (23)$$

---

**Algorithm 1** Iterative algorithm for the C-AES-II method.

---

**Input:**  $N \in \mathbb{N}^+$ ,  $\{\alpha_n\}_{n=1}^N$ ,  $\{\beta_n\}_{n=1}^N$ ,  $\gamma_{n,C-MES}^{th} \in \mathbb{R}^+$ ,  $\bar{\gamma} \in \mathbb{R}^+$ ,  $\varepsilon_{avg} \in (0, 1)$

**Output:**  $\gamma_n^{th} \in \mathbb{R}^+$

```

1:  $n = 1$ 
2:  $\chi = 1$ 
3: while  $\chi = 1$  do
4:   Compute  $\zeta_n$  based on (24)
5:   if  $\zeta_n \geq 0$  then
6:      $\gamma_n^{th} = \zeta_n \gamma_{n,C-MES}^{th}$ 
7:      $\chi = 0$ 
8:   else
9:      $\gamma_n^{th} = 0$ 
10:    if  $n < N$  then
11:       $n = n + 1$ 
12:    else
13:       $\chi = 0$ 
14:    end if
15:  end if
16: end while

```

---

The expression in (23) may provide negative values of  $\zeta_1$  for sufficiently high  $\bar{\gamma}$ . When the average channel quality improves (i.e.,  $\bar{\gamma}$  increases), the average error rate tends to decrease. The value of  $\zeta_1$  then decreases in order to increase the chances of transmitting at lower SNR values and compensate for the error rate reduction so that the average target  $\varepsilon_{avg}$  is met. For values of  $\bar{\gamma}$  beyond certain point, a negative value of  $\zeta_1$  can still meet the required  $\varepsilon_{avg}$  numerically, although this is not possible in practice. Hence, the value of  $\lambda$  in (21a) is selected as  $\lambda = \max(0, \zeta_1)$ .

Motivated by the previous observation, a second strategy, referred to as C-AES-II, is proposed based on an iterative version of C-AES-I (see Algorithm 1). A generalised version of  $\zeta_1$ , as shown in (24), is employed to progressively reduce the SNR threshold for higher MCS when doing so for lower MCS is not enough to meet the desired average error rate. The process starts with the first MCS (line 1) so that in the first iteration of the algorithm the calculation of  $\zeta_n$  based on (24) (line 4) is equivalent to calculate  $\zeta_1$  from (23). If the obtained  $\zeta_1$  is positive (line 5) then the resulting threshold  $\gamma_1^{th}$  from line 6 will be positive as well (i.e., valid) and the algorithm will stop (line 7). In this case the output is the same as for the C-AES-I method. However, if the obtained  $\zeta_1$  from line 4 is negative, the resulting threshold  $\gamma_1^{th}$  from line 6 would be negative as well, which is not a valid value for an SNR threshold. In such case the value for the first threshold is set to zero ( $\gamma_1^{th} = 0$  in line 9) and the algorithm proceeds to the next MCS (line 11). The process is repeated for the next MCS until either an MCS is found such that the SNR threshold obtained from line 6 is positive and therefore valid (in this case the algorithm stops in line 7), or the evaluation of line 10 indicates that no more MCS are available (in this other case the algorithm stops in line 13 with all SNR thresholds set to zero, which leads to the fixed use of the highest MCS available). In this way this method iteratively decreases the SNR thresholds in increasing order to ensure that the target average error rate is met.

$$\zeta_n \approx -\frac{\bar{\gamma}}{\gamma_{n,C-MES}^{th}} \ln \left\{ \frac{1}{1 - \varepsilon_{avg}} \left( \exp \left( -\frac{\gamma_{n,C-MES}^{th}}{\bar{\gamma}} \right) (\varepsilon_{avg} - \bar{\varepsilon}_{C-MES}(\bar{\gamma})) + \exp \left( \frac{1 - 2\alpha_n\beta_n\bar{\gamma}}{2\alpha_n^2\bar{\gamma}^2} \right) \left[ 1 - \varepsilon_n \left( \gamma_{n,C-MES}^{th} + \frac{1}{\alpha_n^2\bar{\gamma}} \right) \right] \right) \right\} \quad (24)$$

300 6.4. Constrained Optimum Error Strategy (C-OES)

The main motivation for error-oriented methods is to limit the experienced error rates in order to avoid frequent retransmissions that would lead to a degraded delay performance. This suggests that the lowest average error rate would lead to the lowest average transmission delay. However, a detailed analysis of (11) reveals that this may not always be true. Under high SNR conditions the probability of transmission is nearly one ( $\bar{\gamma} \gg \gamma_1^{th}$ ) and the average gross data rate  $\bar{R}(\bar{\gamma})$  takes high values close to  $R_N$  owing to the use of high-order MCS. Under such conditions, and according to (11), the average delay can be minimised by minimising the average error rate. However, under low SNR conditions low-order MCS are used more frequently. In such a case, the lowest MCS available and its SNR threshold greatly determines the delay performance since all the parameters involved in (11) are highly dependent on it. If  $\gamma_1^{th}$  decreases,  $p_{tx}(\bar{\gamma})$  increases, which results in a reduction of the delay  $\tau(\bar{\gamma})$ . However, a reduction of  $\gamma_1^{th}$  also decreases  $\bar{R}(\bar{\gamma})$  and increases  $\bar{\varepsilon}(\bar{\gamma})$ , which results in an increase of the delay  $\tau(\bar{\gamma})$ . This observation indicates the existence of a certain value of  $\gamma_1^{th}$  that provides an optimum trade-off among  $p_{tx}(\bar{\gamma})$ ,  $\bar{R}(\bar{\gamma})$  and  $\bar{\varepsilon}(\bar{\gamma})$  that minimises the delay under low SNR conditions. Since in error-oriented methods  $\gamma_1^{th}$  is computed based on the target error rate, this implies the existence of an optimum target error rate (not necessarily the lowest one) that minimises the delay under low SNR. The objective of the C-OES method is to select the SNR thresholds so as to achieve such optimum error rate.

The optimum error rate can be specified in terms of the maximum error rate  $\varepsilon_{max}$  for C-MES, or the average error rate  $\varepsilon_{avg}$  for C-AES. Given the complexity of the expressions involved in (3)–(5) and the varying probabilities of utilisation of each MCS under fading, the analytical derivation of the optimum  $\varepsilon_{max}$  value that would lead the C-MES method to minimise the delay appears to be infeasible, at least without resorting to approximations that would degrade significantly the accuracy (and practical utility) of the resulting expression. On the other hand, it is possible to determine the optimum value of the  $\varepsilon_{avg}$  parameter for the proposed C-AES methods that minimises the delay. It can be shown that  $\bar{R}(\bar{\gamma})$  is not significantly affected by individual variations in the value of  $\gamma_1^{th}$  since  $R_n > R_1, \forall n > 1$ . Given that C-AES meets the target  $\varepsilon_{avg}$  by readjusting  $\gamma_1^{th}$  and  $\partial \bar{R}(\bar{\gamma}) / \partial \gamma_1^{th} \approx 0$ , it hence holds that  $\partial \bar{R}(\bar{\gamma}) / \partial \varepsilon_{avg} \approx 0$ ; therefore minimising the delay is equivalent to minimising  $1/p_{tx}(\bar{\gamma}) [1 - \bar{\varepsilon}(\bar{\gamma})]$ , or maximising  $p_{tx}(\bar{\gamma}) [1 - \bar{\varepsilon}(\bar{\gamma})]$ . The desired  $\varepsilon_{avg}$  can thus be found by solving the equation  $\partial p_{tx}(\bar{\gamma}) [1 - \bar{\varepsilon}(\bar{\gamma})] / \partial \varepsilon_{avg} = 0$ , which requires first expressing  $p_{tx}(\bar{\gamma})$  and  $\bar{\varepsilon}(\bar{\gamma})$  as a function of  $\varepsilon_{avg}$ .

In the term  $p_{tx}(\bar{\gamma}) = \exp(-\gamma_1^{th}/\bar{\gamma})$ , the SNR threshold is calculated by C-AES as  $\gamma_1^{th} = \zeta_1 \gamma_{1,C-MES}^{th}$ , where  $\zeta_1$  is given by (23) and  $\gamma_{1,C-MES}^{th} = (1/\alpha_1)[\beta_1 + \mathcal{Q}^{-1}(\varepsilon_{avg})]$  is obtained using (20) with  $\varepsilon_{max} = \varepsilon_{avg}$ . Introducing these equalities into (2) yields:

$$p_{tx}(\bar{\gamma}) = \frac{1}{1 - \varepsilon_{avg}} \left( \exp \left( -\frac{\gamma_{1,C-MES}^{th}}{\bar{\gamma}} \right) (\varepsilon_{avg} - \bar{\varepsilon}_{C-MES}(\bar{\gamma})) + \exp \left( \frac{1 - 2\alpha_1\beta_1\bar{\gamma}}{2\alpha_1^2\bar{\gamma}^2} \right) \left[ 1 - \varepsilon_1 \left( \gamma_{1,C-MES}^{th} + \frac{1}{\alpha_1^2\bar{\gamma}} \right) \right] \right) \quad (25)$$

Since  $\bar{\varepsilon}_{C-MES}(\bar{\gamma}) \ll \varepsilon_{max} = \varepsilon_{avg}$ , the approximation  $\varepsilon_{avg} - \bar{\varepsilon}_{C-MES}(\bar{\gamma}) \approx \varepsilon_{avg}$  is valid, which removes  $\bar{\varepsilon}_{C-MES}(\bar{\gamma})$  from the equation. The terms that depend on  $\gamma_{1,C-MES}$  (and therefore on  $\varepsilon_{avg}$ ) can be expressed in a more convenient form using the logistic/sigmoid approximations  $\mathcal{Q}(x) \approx 1/(1 + \exp(\kappa x))$  and  $\mathcal{Q}^{-1}(x) \approx \ln((1/x) - 1)/\kappa$ , where  $\kappa = 1.7$  is the optimum fitting coefficient that numerically minimises the approximation error. Hence:

$$\exp \left( -\frac{\gamma_{1,C-MES}^{th}}{\bar{\gamma}} \right) \approx \exp \left( -\frac{\beta_1}{\alpha_1\bar{\gamma}} \right) \left( \frac{\varepsilon_{avg}}{1 - \varepsilon_{avg}} \right)^{\frac{1}{\kappa\alpha_1\bar{\gamma}}} \quad (26)$$

$$\varepsilon_1 \left( \gamma_{1,C-MES}^{th} + \frac{1}{\alpha_1^2\bar{\gamma}} \right) \approx \frac{1}{1 + \exp \left( \frac{\kappa}{\alpha_1\bar{\gamma}} \right) \left( \frac{1 - \varepsilon_{avg}}{\varepsilon_{avg}} \right)} \quad (27)$$

Introducing (26) and (27) into (25) leads to:

$$p_{tx}(\bar{\gamma}) \approx \exp\left(-\frac{\beta_1}{\alpha_1 \bar{\gamma}}\right) \left(\frac{\varepsilon_{avg}}{1 - \varepsilon_{avg}}\right)^{1 + \frac{1}{\kappa \alpha_1 \bar{\gamma}}} + \frac{\exp\left(\frac{1 - 2\alpha_1 \beta_1 \bar{\gamma}}{2\alpha_1^2 \bar{\gamma}^2}\right)}{1 - \varepsilon_{avg}} \left(1 - \frac{1}{1 + \exp\left(\frac{\kappa}{\alpha_1 \bar{\gamma}}\right) \left(\frac{1 - \varepsilon_{avg}}{\varepsilon_{avg}}\right)}\right) \quad (28)$$

The objective function  $p_{tx}(\bar{\gamma}) [1 - \bar{\varepsilon}(\bar{\gamma})]$  can be expressed in terms of  $\varepsilon_{avg}$  by using (28) along with  $\bar{\varepsilon}(\bar{\gamma}) = \varepsilon_{avg}$  (notice that C-AES methods are designed to meet the specified target error rate  $\varepsilon_{avg}$ ). The equation resulting from  $\partial p_{tx}(\bar{\gamma}) [1 - \bar{\varepsilon}(\bar{\gamma})] / \partial \varepsilon_{avg} = 0$  can be solved for  $\varepsilon_{avg}$  by assuming  $\alpha_1 \bar{\gamma} \gg \kappa$ , which is valid in practical conditions<sup>3</sup>, leading to the approximated result:

$$\varepsilon_{avg}^* \approx 1 - 2Q\left(\frac{1}{\alpha_1 \bar{\gamma}}\right) \quad (29)$$

Notice that the optimum value of  $\varepsilon_{avg}$  that minimises the delay for C-AES,  $\varepsilon_{avg}^*$ , depends not only on the most robust MCS,  $\alpha_1$ , but also on the average channel quality,  $\bar{\gamma}$ . In particular, for high SNR the delay is minimised when a low average error rate is achieved ( $\lim_{\bar{\gamma} \rightarrow \infty} \varepsilon_{avg}^* = 0$ ); however, the minimisation of the delay under low SNR conditions is accomplished by aiming at large average error rates ( $\lim_{\bar{\gamma} \rightarrow 0} \varepsilon_{avg}^* = 1$ ). The operating principle of the C-OES method is to compute the value of the optimum error rate  $\varepsilon_{avg}^*$  for the current average SNR  $\bar{\gamma}$  based on (29) and then employ C-AES in order to meet the obtained  $\varepsilon_{avg}^*$  target.

### 6.5. Constrained Minimum Delay and Minimum Energy Consumption Strategies

As pointed out in Section 5.3 for unconstrained methods, the strategies of maximising the throughput, minimising the delay and minimising the energy consumption lead to the same set of SNR thresholds for AMC. A similar conclusion can be reached for the constrained versions of these methods. Following a similar approach as in Section 6.1, the *cut-off* SNR threshold can be set by imposing a limit on the maximum instantaneous delay/energy consumption of the lowest MCS, rather than its minimum instantaneous throughput. Concretely,  $\gamma_1^{th}$  can be set at the SNR value where the delay/energy consumption of the first MCS does not exceed the minimum achievable value by more than a fraction  $\psi \in (0, 1)$ . Hence,  $\gamma_1^{th}$  is obtained by solving the equation  $R_N / \{R_1 [1 - \varepsilon_1(\gamma_1^{th})]\} = (1 + \psi) R_N / R_1$ , which yields  $\gamma_1^{th} = \varepsilon_1^{-1}(\psi / (1 + \psi))$ . While this expression is different from (18a) (the rest of SNR thresholds are equal), both are equivalent since  $\xi = 1 / (1 + \psi)$ . Therefore, the *cut-off* SNR threshold obtained by imposing a certain constraint on the maximum delay/energy consumption of the lowest MCS can also be obtained by imposing an equivalent constraint on its minimum throughput, thus confirming that these strategies provide the same set of SNR thresholds for AMC.

## 7. Numerical Results

Table 1 summarises the SNR threshold-setting methods presented and discussed in Sections 5 and 6. For each method, the table shows the section where it is discussed, the equation employed to calculate the SNR thresholds (or alternatively the algorithm or external reference) and an indication of whether it is an existing method in the literature proposed by other authors (E), a novel method proposed in this work (P) or an adaptation of an existing principle to the scope of this work (A).

The performance of the SNR threshold-setting strategies formulated in Sections 5 and 6 is comparatively assessed in this section by numerically evaluating the performance models derived in Section 4. Such performance models were validated with results from a simulator specifically created to that end, showing an excellent level of accuracy. For the sake of clarity, the figures presented in this section only include

<sup>3</sup>When the model of (1) is fitted to MCS that provide low error rates (i.e. robust MCS),  $\alpha_n$  takes high values and  $\alpha_1 \bar{\gamma} \gg \kappa$  is true for practical average SNR values. For example, fitting (1) to the MCS of LTE [33, Fig. 5] leads to  $\alpha_1 = 39.64$ , hence  $\alpha_1 \bar{\gamma} \gg \kappa$  implies  $10 \log_{10} \bar{\gamma} \gg -13.68$  dB. An average SNR 3 dB greater than (i.e., two times) this value is enough to make this approximation valid.

Table 1: Summary of SNR threshold-setting methods considered in this work.

Target	Unconstrained				Constrained			
	Name	Section	Equation	E/P/A	Name	Section	Equation	E/P/A
Throughput	U-MTS	5.1	(16)	E	Mode 0	6.1	Ref. [16]	E
					C-MTS-I	6.1	(18)	P
					C-MTS-II	6.1	(19)	P
Error	U-MES	5.2	(17)	E	C-MES	6.2	(20)	E
					C-AES-I	6.3	(21)	P
					C-AES-II	6.3	Algorithm 1	P
Delay	N/A	5.3	(16)	A	C-OES	6.4	C-AES-II with (29)	P
Energy	N/A	5.3	(16)	A	N/A	6.5	(18)–(19)	A

E: Existing in the literature / P: Proposed in this work / A: Adaptation of existing principle.

numerical results. For evaluation purposes, the MCS defined by the LTE standard are here considered [33, Fig. 5]. Notice that the *mode 0* method proposed in [16] is based on a network level approach that takes into account the presence of several users and the varying channel quality conditions as a result of mutual interference relations and packet retransmissions. Such network level approach is out of the scope of this work, where the focus is on the link level. Therefore, the *mode 0* method is not included in the subsequent comparative analysis (however, a detailed performance evaluation from a network level perspective can be found in [35]).

### 7.1. Throughput-Oriented Methods

This section evaluates and compares the methods aimed at maximising the throughput (i.e., U-MTS, C-MTS-I and C-MTS-II). Fig. 2 compares the throughput performance of these methods (expressed in bits per second per LTE physical resource block). As it can be appreciated, U-MTS provides the highest throughput over the whole range of average SNR values. However, this unconstrained method makes a continuous use of the channel (i.e.,  $p_{tx}(\bar{\gamma}) = 1$ ) as shown in Fig. 3, even when the channel quality is poor and the experienced throughput is nearly zero. To prevent this inefficient use of radio resources, the constrained versions of the MTS method are intended to restrict the use of the channel during periods of momentary degraded performance (by imposing a limit on the minimum instantaneous SNR below which transmission is temporarily ceased) so that the channel can temporally be accessed by other users under better transmission conditions, who would make a more efficient use thereof. The ultimate objective is to minimise the degree to which the channel is used without incurring in a noticeable performance degradation with respect to the U-MTS method. The C-MTS-II method attempts to achieve this goal by forcing a constant probability of transmission  $\rho < 1$ , which is effectively met over the whole range of SNR values as shown in Fig. 3. However, this approach leads to a noticeable throughput performance degradation: with C-MTS-II the user transmits a fraction  $\rho < 1$  of the time and the experienced throughput decreases by a similar proportion with respect to the case  $\rho = 1$  (i.e., U-MTS). While the absolute throughput difference with respect to U-MTS (shown in the bottom of Fig. 2) is negligible under low SNR conditions, it constitutes a noticeable performance degradation in the region of high SNR values. This undesired behaviour is a consequence of forcing a constant probability of transmission, which always prevents the user from transmitting in a fraction  $1 - \rho$  of the slots, even when the channel quality experienced in that bottom  $1 - \rho$  is sufficiently good to yield a significant throughput. On the other hand, the results obtained for the C-MTS-I method indicate that it is able to significantly reduce the degree to which the channel is used (Fig. 3) without a noticeable throughput performance degradation with respect to U-MTS (Fig. 2). While the C-MTS-I probability of transmission is close to one for high SNR values, it is drastically reduced under poor channel conditions. For instance, at average SNR values of 0, -5 and -10 dB, the C-MTS-I method is able to achieve a similar throughput compared to the U-MTS method but making use of the channel 87-89%, 65-71%, and 26-33% of the time, respectively (i.e., only when the instantaneous channel quality is good enough for the

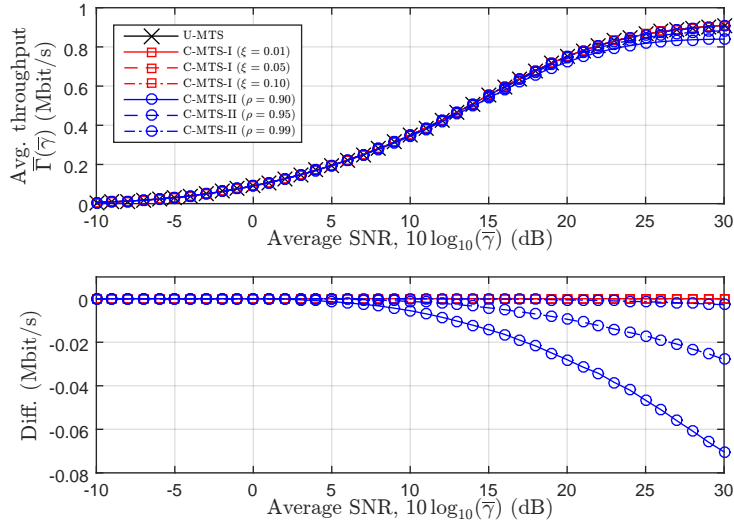


Figure 2: Average throughput as a function of the average SNR.

transmission to be beneficial). For the remaining time the channel can be accessed by other users under better transmission conditions, thus providing a significant throughput and capacity improvement at the system level with respect to U-MTS without noticeable individual performance degradation at the link level.

410 Fig. 4 compares the average normalised delay of the throughput-oriented methods based on (11), where a constant error probability across retransmissions is assumed. While the delay performance of the C-MTS-II method is similar (low SNR) or slightly higher (high SNR) than that of the U-MTS method, C-MTS-I results in a similar delay for high SNR values and a noticeably lower delay under low SNR conditions (about 14-18% lower at an average SNR of -5 dB and 8-10% lower at an average SNR of -10 dB). The lower delay of the  
 415 C-MTS-I method under low SNR conditions can be explained as follows. The U-MTS method always allows user transmissions no matter how low the SNR is. Under low SNR conditions, U-MTS selects MCS with a higher amount of redundant bits and therefore a lower amount of information bits,  $B_u$ . If the transmitted packet is received in error, which is likely when the SNR is low, a retransmission will be performed in the next slot; however, this packet size may not be optimum in the next slot if the SNR allows the use of a higher  
 420 MCS with a greater number of information bits. By contrast, in the same scenario the C-MTS-I method would prevent the transmission in the first slot and allow the transmission in the second slot, when the SNR is higher, thus selecting a higher MCS with a higher amount of information bits,  $B_c > B_u$ . In this example U-MTS and C-MTS-I would correctly transmit  $B_u$  and  $B_c > B_u$  bits, respectively, in two slots, which would lead to a higher throughput and therefore a lower number of transmissions required for a certain volume of  
 425 data (i.e., a lower delay) in the case of C-MTS-I<sup>4</sup>, as it can be appreciated in Fig. 4. Moreover, C-MTS-I also leads to a lower average error rate owing to the transmission restrictions under poor channel quality conditions. This lower error rate implies a lower retransmission probability and consequently a significantly lower energy consumption as observed in Fig. 5 (e.g., energy consumption is about 40-46% lower at an average SNR of -5 dB and 70-77% lower at -10 dB).

430 In summary, the obtained results indicate that the proposed C-MTS-I method can significantly reduce the degree to which a channel is used without a significant throughput performance degradation with respect to its unconstrained counterpart (i.e., U-MTS). This attractive feature allows other users under better

<sup>4</sup>The results shown in Fig. 2 are based on (7), which does not capture the impact of using the same MCS for retransmissions (i.e., the optimum MCS is selected in every slot). Hence, no throughput difference is observed in Fig. 3 between U-MTS and C-MTS-I. However, results obtained from simulations confirmed the existence of such difference, although it is not very significant in practice (hence the selection of results shown in Fig. 2).

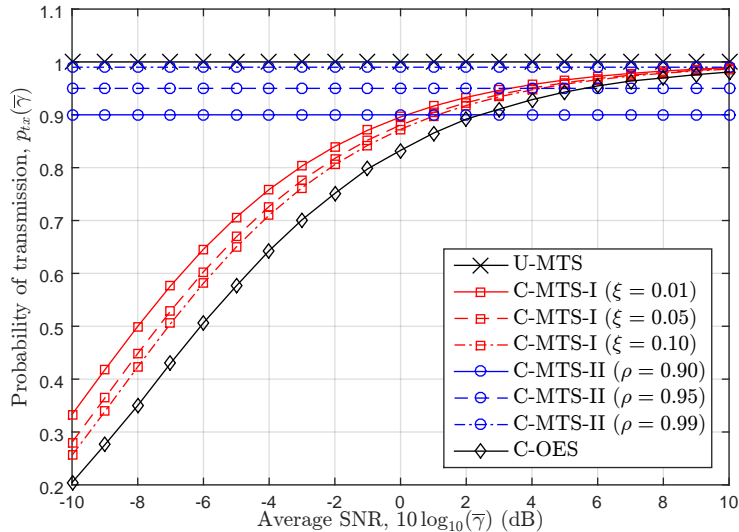


Figure 3: Probability of transmission as a function of the average SNR.

transmission conditions to temporarily access the same channel, thus providing a significant throughput and capacity improvement at the system level with respect to U-MTS without noticeable individual performance degradation at the link level. Moreover, C-MTS-I outperforms U-MTS in terms of delay and energy consumption. These features make the proposed C-MTS-I method an attractive option for AMC.

## 7.2. Error- and Delay-Oriented Methods

This section evaluates and compares the methods aimed at meeting a specific target error rate (i.e., U-MES, C-MES, C-AES-I and C-AES-II) and minimising the delay (i.e., C-OES). Fig. 6 compares the average error rate for the error-oriented methods. A group of three curves is shown for each method, corresponding to target error rates of 0.01 (bottom), 0.05 (middle) and 0.10 (top). The target of the MES methods is to guarantee that a maximum error rate  $\varepsilon_{max}$  is not exceeded. As it can be appreciated in Fig. 6, the unconstrained version of this method (i.e., U-MES) is unable to meet this objective (the average error rate  $\bar{\varepsilon}(\bar{\gamma})$  is greater than the desired instantaneous maximum  $\varepsilon_{max}$ ); this is due to the lack of transmission constraints with U-MES, which leads to high error rates under poor channel quality conditions. Notice that the average error rate experienced with U-MES is nearly independent of the target  $\varepsilon_{max}$  (except for high SNR values, where the values of  $\bar{\varepsilon}(\bar{\gamma})$  are lower than 0.01 and the differences are not very significant). On the other hand, by preventing transmissions under low SNR conditions, the constrained version of this method (i.e., C-MES) is able to guarantee that the desired maximum  $\varepsilon_{max}$  is never exceeded<sup>5</sup>, which results in low average error rates as shown in Fig. 6. As opposed to U-MES, the target error rate  $\varepsilon_{max}$  has a more noticeable impact on the C-MES error performance. Thus, only the constrained version of the MES method can effectively control the experienced error rates and guarantee that the target maximum error rate  $\varepsilon_{max}$  is never exceeded.

The C-AES methods are designed to control the average error rate rather than its maximum value. As shown in Fig. 6, the C-AES-I method can closely meet the target average error rate  $\varepsilon_{avg}$  on a certain range of SNR values. Recall that the target  $\varepsilon_{avg}$  is met by C-AES-I by readjusting the SNR threshold  $\gamma_1^{th}$  of the C-MES method by a factor  $\zeta_1$  given by (23). As the average channel quality (i.e.,  $\bar{\gamma}$ ) increases, the average error rate tends to decrease and the value of  $\zeta_1$  decreases in order to increase the chances of transmitting

<sup>5</sup>While results for the maximum error rate are not shown, the ability of the C-MES method to meet the target  $\varepsilon_{max}$  is evident given the formulation of the method itself.

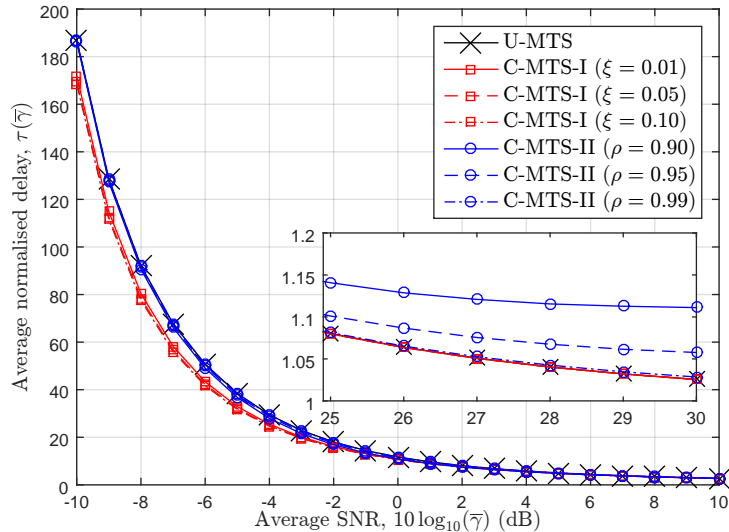


Figure 4: Average normalised delay as a function of the average SNR (throughput-oriented methods).

at lower SNR and compensate for the error rate reduction so that the target  $\varepsilon_{avg}$  is met. There is a certain value of  $\bar{\gamma}$  for which  $\zeta_1 = 0$  (i.e.,  $\gamma_1^{th} = 0$ ); beyond that point all SNR thresholds are identical for C-AES-I and U-MES and therefore both methods exhibit the same average error performance as appreciated in Fig. 6. By readjusting in a similar manner the SNR thresholds  $\gamma_n^{th}$  for higher MCS ( $n > 1$ ), the C-AES-II method is able to closely meet the desired  $\varepsilon_{avg}$  at higher average SNR values as well (the observed *sawtooth* shape is a natural consequence of the iterative algorithm of Fig. 1). When the average SNR is sufficiently high, only the highest MCS ( $n = N$ ) is employed and the average error rate is then dominated by  $\bar{\varepsilon}_N(\bar{\gamma})$ ; in such a case it is not possible to meet the desired error rate any more, which explains  $\bar{\varepsilon}(\bar{\gamma}) \ll \varepsilon_{avg}$  for C-AES-II under very high SNR.

It is worth mentioning that the accuracy of the approximations employed to analytically derive  $\zeta_1$  and  $\zeta_n$  in (23) and (24), respectively, degrades for very low values of  $\bar{\gamma}$ . As a result, the analytical calculation of  $\zeta_1$  and  $\zeta_n$  for C-AES-I and C-AES-II cannot accurately meet the desired  $\varepsilon_{avg}$  under very low SNR as appreciated in Fig. 6. The exact values required for  $\zeta_1$  and  $\zeta_n$  could be obtained by solving (22) numerically, which would guarantee that the requirement  $\bar{\varepsilon}(\bar{\gamma}) = \varepsilon_{avg}$  is met for any arbitrary SNR. However, taking into account the range of average SNR values in real LTE systems, the results in (23) and (24) are accurate under practical operation conditions.

An important motivation to control the (maximum or average) error rate is to avoid frequent retransmissions that would degrade the delay performance. This is particularly important in delay-sensitive services or systems designed to provide low latency such as LTE (as a matter of fact, the LTE standard employs C-MES with  $\varepsilon_{max} = 0.10$  [36, Sec. 7.2.3]). As discussed in Section 6.4, the optimum error rate that minimises the delay is not necessarily the lowest possible one. This is illustrated in Fig. 7 for both C-MES and C-AES methods, where the normalised delay is shown as a function of the  $\varepsilon_{max}$  and  $\varepsilon_{avg}$  parameters, respectively, along with their optimum values as a function of the average SNR. As it can be appreciated, the delay experienced at low (high) SNR can be minimised by aiming at high (low) error rates, i.e., targeting a low error rate is not always optimum in terms of delay. Notice that the target  $\varepsilon_{max} = 0.10$  specified by the LTE standard leads to a nearly optimum delay with C-MES for high SNR values. However, under poor channel quality conditions, such target error rate is far from minimising the delay. A similar dependence on the average SNR is observed for the  $\varepsilon_{avg}$  parameter of C-AES. While the optimum value of  $\varepsilon_{max}$  that minimises the C-MES delay can be computed numerically, the analytical derivation of a closed-form relation between both parameters appears to be infeasible as discussed in Section 6.4, which motivates the proposed C-AES



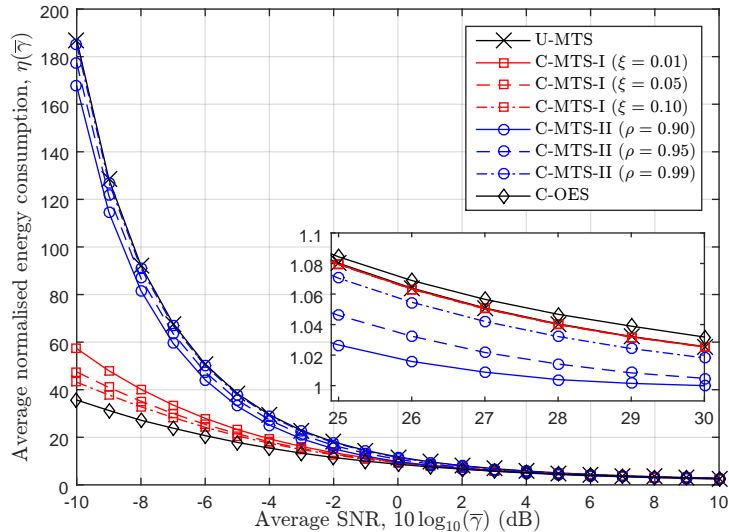


Figure 5: Average normalised energy consumption as a function of the average SNR.

methods. For the C-AES methods it is possible to express the experienced delay as a function of the  $\varepsilon_{avg}$  parameter, which enables the analytical derivation of the optimum value for  $\varepsilon_{avg}$ . As observed in Fig. 7, the analytical result of (29) provides an accurate estimation of the true optimum  $\varepsilon_{avg}$  value.

Fig. 8 compares the delay performance of throughput-oriented methods (U-MTS and C-MTS-I), error-oriented methods (U-MES, C-MES and C-AES-II) and delay-oriented methods (C-OES based on C-AES-II). In general, unconstrained methods lead to higher delays due to the higher error rates resulting from the lack of transmission constraints, while their constrained counterparts lead to lower delays. Different methods lead to different delay performances (depending on their configuration parameters) and can provide a nearly optimum delay over certain limited SNR regions. However, only the proposed C-OES method is able to provide the minimum possible delay over the whole range of SNR values, which is a consequence of its channel-dependent adaptive target error rate. It is also interesting to compare the performance of the proposed C-OES method and the C-MES method with  $\varepsilon_{max} = 0.10$  used by the LTE standard. As it can be appreciated in Fig. 8, both methods provide an optimum delay under high SNR conditions (which in fact is true for all methods). As the SNR decreases, the delay performance degrades for both methods. However, the performance of the AMC method employed by the LTE standard degrades to a more significant extent compared to the proposed C-OES method (e.g., the delay is about 31% higher at an average SNR of -10 dB). These results demonstrate the ability of the proposed C-OES method to significantly reduce the experienced delay under low SNR conditions, thus providing an optimum delay performance over the entire range of SNR values.

In terms of throughput performance, the C-OES method was observed to be very similar to the C-MTS-I method (shown in Fig. 2), which based on the analysis of Section 7.1 can be considered as the most convenient option when the objective is the throughput maximisation. As a matter of fact, both methods provide a nearly identical throughput and delay performance (as appreciated in Fig. 8). However, the C-OES method was observed to attain such performance more efficiently, making use of the channel to a notable lower extent (see Fig. 3) and consuming an appreciable lower amount of energy (see Fig. 5). In particular, C-OES reduces the probability of transmission (i.e., channel usage) by up to 17-38% and the energy consumption by up to 20-39% with respect to C-MTS-I, which represents a noticeable further improvement compared to the U-MTS method (i.e., the method providing the maximum throughput). Although the C-OES method was originally conceived to minimise the delay, the obtained results demonstrate that it can also provide an optimum throughput performance with a significantly lower channel usage and energy consumption compared to other popular SNR threshold-setting methods for AMC.

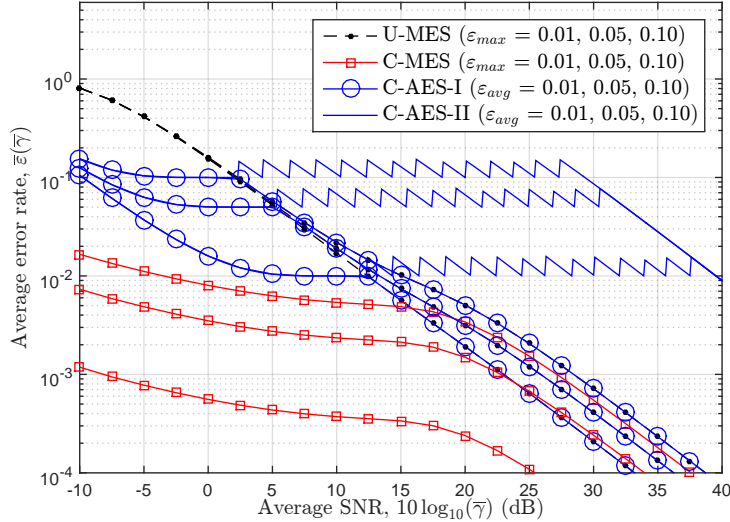


Figure 6: Average error rate as a function of the average SNR.

## 8. Discussion

As discussed in Section 1, this work considers a technology- and service-agnostic approach, where particular features of specific radio technologies or services are not taken into account, and abstracted wherever required. However, as with any other technique, the use of AMC in a practical context unavoidably requires the consideration of features and constraints that are specific to the scenario of application, which may require some adaptation of the AMC principles to the considered radio technology or service.

An example is the case of LTE, which is based on Orthogonal Frequency-Division Multiplexing (OFDM), where each subcarrier may experience a different SNR but the MCS needs to be selected per Physical Resource Block (PRB), which typically includes 12 subcarriers. A similar problem may be found in Multiple-Input and Multiple-Output (MIMO) systems, where each antenna may experience a different SNR and the MCS selection may be performed jointly considering all SNR values. The methods considered in this work, which have been analysed considering a single SNR value, could be readily applied to these multiple-SNR scenarios by weighting the different SNR values to produce a single *effective* SNR, which would then be used to select the optimum MCS. Alternatively, the same principles could be used to calculate the (multidimensional) region of SNR values where each MCS would be selected; however, such calculation is likely to be complex and require numerical optimisation methods. In MIMO OFDM scenarios, the MCS is typically selected based on an optimisation process that takes into account the SNR of each individual signal stream (i.e., OFDM subcarrier and/or MIMO antenna) and selects the MCS so as to optimise a predefined target performance metric such as throughput, error, delay, energy, or a combination thereof. While the literature on AMC in the context of MIMO OFDM is abundant, most existing work essentially considers the throughput maximisation (U-MTS) and/or error-oriented (U-MES/C-MES) principles [37, 38, 39], which are the most widely used methods, even though energy efficiency is sometimes considered as well [40]. The study of AMC can be further particularised by taking into account aspects that are specific to the considered type of communication network, such as for example relay networks [41], Ultra-Reliable and Low-Latency Communication (URLLC) 5G networks [42] and Visible Light Communication (VLC) networks [43].

The motivation for the generic technology- and service-agnostic approach considered in this work is to focus on the essence of the principles commonly used to adaptively select the MCS (and propose new ones as well), removing any potential bias that might be introduced by the consideration of particular features or constraints from specific radio technologies or services that may not be widely applicable in other scenarios. Consequently, the new methods proposed in this work (as it is the case for other existing methods in the

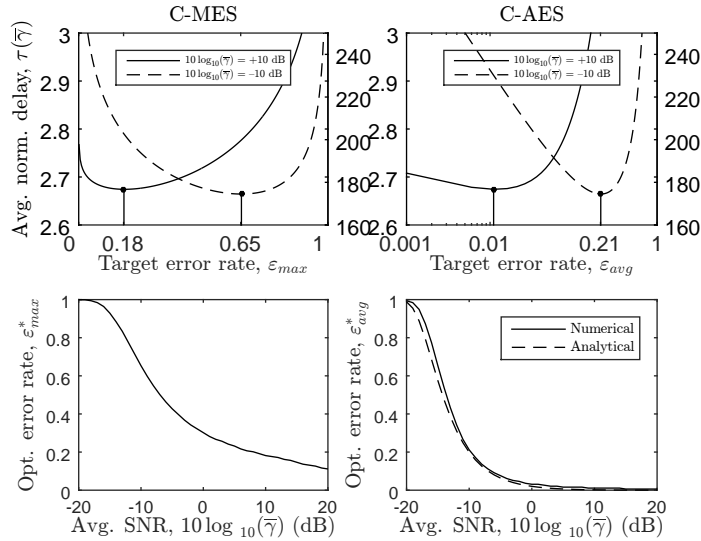


Figure 7: Average normalised delay as a function of the target error rate parameter (top) and its optimum value as a function of the average SNR (bottom) for C-MES (left) and C-AES (right).

550 literature as well) may require some adaptation for the application to specific scenarios. In this context, the particularisation of the new methods proposed in this work in the context of MIMO OFDM is an interesting aspect that requires further investigation and is suggested as future work.

## 9. Conclusions

555 AMC is commonly used in wireless communication systems to dynamically adapt the employed MCS to the instantaneous channel quality (typically expressed in terms of the instantaneous SNR) based on a set of SNR thresholds, which define the range of SNR values on which each MCS is employed. This work has performed a detailed and rigorous analysis of SNR threshold-setting strategies for AMC, not only considering conventional methods commonly used in the literature but also proposing new methods to attain specific performance targets in terms of error rate, delay and spectral/energy efficiency. The obtained results 560 demonstrate that the proposed methods provide significant improvements in terms of error rate, delay and spectral/energy efficiency with respect to traditional methods commonly used in the existing literature (and adopted by several communication standards). In particular, the C-OES method has been proposed in this work to minimise the delay by targeting a specific optimum error rate, which depends on the experienced channel quality. Compared to the popular error-oriented AMC method based on a fixed target error rate, the proposed C-OES method can provide significant delay performance improvements under low SNR conditions, thus leading to an optimum delay performance for any arbitrary SNR. Compared to the popular throughput-oriented AMC method based on the throughput maximisation, the proposed C-OES method not only is more energy-efficient but also reduces significantly the degree to which the channel is used without a noticeable throughput performance degradation (thus leading to significant capacity improvements at the system level without noticeable individual performance degradation at the link level). These appealing features make of 570 the proposed C-OES method an excellent option for AMC.

## Appendix

The expression for the average number of transmissions in (10) assumes infinite retransmissions and a constant probability of error across (re)transmissions. In practice, some systems may allow a maximum of

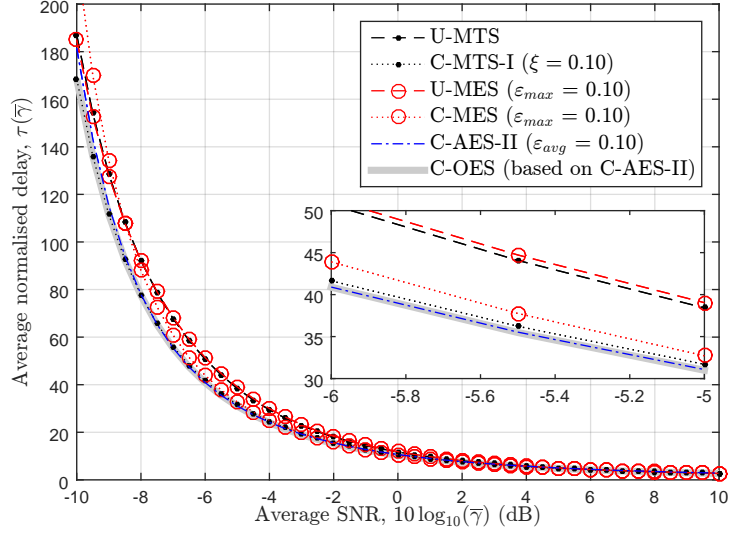


Figure 8: Average normalised delay as a function of the average SNR (selected methods).

575  $K$  transmissions in total, whereupon the packet is discarded. In such a case, the expression for the average number of transmissions is given by:

$$\bar{\nu}(\bar{\gamma}) = \sum_{k=1}^K p_k(\bar{\gamma}) k = [1 - \bar{\varepsilon}(\bar{\gamma})] \sum_{k=1}^K k [\bar{\varepsilon}(\bar{\gamma})]^{k-1} = \frac{1 + K [\bar{\varepsilon}(\bar{\gamma})]^{K+1} - (K+1) [\bar{\varepsilon}(\bar{\gamma})]^K}{1 - \bar{\varepsilon}(\bar{\gamma})} \quad (30)$$

580 which reduces to (10) when  $K \rightarrow \infty$ . Moreover, the error probability may vary across retransmissions. One possible reason is the combination of retransmissions of the same packet to increase the probability of correct reception (e.g., Chase combining or incremental redundancy techniques), which can be modelled as a shift of the error probability curves (equivalently, an increase of the effective SNR) in every new retransmission [33, Fig. 6], thus leading to:

$$\bar{\nu}(\bar{\gamma}) = \sum_{k=1}^K k \left( \prod_{l=0}^{k-1} \xi_l(\bar{\gamma}) \right) [1 - \bar{\varepsilon}(\bar{\gamma} + \Delta\bar{\gamma}_{k-1})] \quad (31)$$

585 where  $\Delta\bar{\gamma}_k$  represents the effective SNR increment in the  $k$ th retransmission (i.e.,  $(k+1)$ th transmission), with  $\Delta\bar{\gamma}_0 = 0$ , and  $\xi_l(\bar{\gamma})$  is defined as  $\xi_l(\bar{\gamma}) = 1$  for  $l = 0$  and  $\xi_l(\bar{\gamma}) = \bar{\varepsilon}(\bar{\gamma} + \Delta\bar{\gamma}_{l-1})$  for  $l \geq 1$ . Another possible reason is an increased level of interference due to retransmissions, which can be modelled by replacing  $\bar{\gamma}$  with an effective value given by [16, eq. (4)]:

$$\bar{\gamma}_{eff} = \frac{\bar{\gamma}}{\sum_{n=1}^N \frac{p_n(\bar{\gamma})}{1 - \bar{\varepsilon}_n(\bar{\gamma})/p_{tx}(\bar{\gamma})}} \quad (32)$$

where  $p_n(\bar{\gamma})$  represents the probability of selecting the  $n$ th MCS and is given (under Rayleigh fading) by  $p_n(\bar{\gamma}) = e^{-\gamma_n^{th}/\bar{\gamma}} - e^{-\gamma_{n+1}^{th}/\bar{\gamma}}$  for  $n = 1, \dots, N-1$ , and  $p_n(\bar{\gamma}) = e^{-\gamma_n^{th}/\bar{\gamma}}$  for  $n = N$ .

590 The results of this appendix are provided for completeness of the analysis and can be useful when taking these particular aspects of certain wireless communication systems into account. However, for the purposes of this work (where a more general technology-independent approach is adopted) the expression obtained in (10) is sufficient and constitutes a preferred option.

## References

- [1] K. K. Leung, P. F. Driessen, K. Chawla, X. Qiu, Link adaptation and power control for streaming services in EGPRS wireless networks, *IEEE J. Sel. Areas Commun.* 19 (10) (2002) 2029–2039.
- 595 [2] T. Cui, F. Lu, V. Sethuraman, A. Goteti, S. P. N. Rao, P. Subrahmanya, Throughput optimization in high speed downlink packet access (HSDPA), *IEEE Trans. Wireless Commun.* 10 (2) (2011) 474–483.
- [3] G. Ku, J. Walsh, Resource allocation and link adaptation in LTE and LTE advanced: a tutorial, *IEEE Commun. Surveys Tuts.* 17 (3) (2015) 1605–1633.
- 600 [4] S. Avallone, N. Pasquino, S. Zinno, D. Casillo, Experimental characterization of LTE adaptive modulation and coding scheme under actual operating conditions, in: *Proc. IEEE Int'l. Workshop on Measurement and Networking (M&N 2017)*, Naples, Italy, 2017, pp. 1–6.
- [5] D. Qiao, S. Choi, K. G. Shin, Goodput analysis and link adaptation for IEEE 802.11a wireless LANs, *IEEE Trans. Mobile Comput.* 1 (4) (2002) 278–292.
- 605 [6] P. Chevillat, J. Jelitto, A. N. Barreto, H. Truong, A dynamic link adaptation algorithm for IEEE 802.11 a wireless LANs, in: *Proc. IEEE Int'l. Conf. Commun. (ICC 2003)*, Vol. 2, Anchorage, United States, 2003, pp. 1141–1145.
- [7] Q. Dong, K. Hayashi, M. Kaneko, Adaptive modulation and coding design for communication-based train control systems using IEEE 802.11 MAC with RTS/CTS, in: *Proc. IEEE 18th Int'l. Workshop on Signal Processing Advances in Wireless Communications (SPAWC 2017)*, Vol. 2, Sapporo, Japan, 2017, pp. 1–5.
- 610 [8] F. Martelli, R. Verdone, C. Buratti, Link adaptation in IEEE 802.15.4-based wireless body area networks, in: *Proc. 21st IEEE Int'l. Symp. Pers., Indoor and Mobile Radio Commun. (PIMRC 2010)*, Istanbul, Turkey, 2010, pp. 117–121.
- [9] F. Martelli, R. Verdone, C. Buratti, Link adaptation in wireless body area networks, in: *Proc. 73rd IEEE Veh. Technol. Conf. (VTC 2011 Spring)*, Yokohama, Japan, 2011, pp. 1–5.
- [10] M. S. Mohammadi, E. Dutkiewicz, Q. Zhang, X. Huang, Optimal energy efficiency link adaptation in IEEE 802.15.6 IR-UWB body area networks, *IEEE Commun. Lett.* 18 (12) (2014) 2193–2196.
- 615 [11] D. Marabissi, D. Tarchi, R. Fantacci, F. Balleri, Efficient adaptive modulation and coding techniques for WiMAX systems, in: *Proc. IEEE Int'l. Conf. Commun. (ICC 2008)*, Beijing, China, 2008, pp. 3383–3387.
- [12] C. Mehlführer, S. Caban, M. Rupp, Experimental evaluation of adaptive modulation and coding in MIMO WiMAX with limited feedback, *EURASIP Journal on Advances in Signal Processing* 2008 (837102) (2008) 1–12.
- 620 [13] J. Huang, Y. Su, W. Liu, F. Wang, Adaptive modulation and coding techniques for global navigation satellite system inter-satellite communication based on the channel condition, *IET Comms.* 10 (16) (2016) 2091–2095.
- [14] M. Visintin, G. Montorsi, M. Cossu, N. Jeannin, Algorithms for the implementation of adaptive coding modulation on Earth observation satellites, in: *Proc. IEEE Int'l. Workshop on Tracking, Telemetry and Command Systems for Space Applications (TTC 2016)*, Noordwijk, Netherlands, 2016, pp. 1–8.
- 625 [15] M. López-Benítez, J. Gozávez, Link adaptation algorithms for improved delivery of delay- and error-sensitive packet-data services over wireless networks, *Wireless Networks* 16 (3) (2010) 593–606.
- [16] X. Qiu, J. Chuang, Link adaptation in wireless data networks for throughput maximization under retransmissions, in: *Proc. IEEE Int'l. Conf. Commun. (ICC 1999)*, Vol. 2, Vancouver, Canada, 1999, pp. 1272–1277.
- 630 [17] K. Manolakis, M. A. Gutiérrez-Estévez, V. Jungnickel, Adaptive modulation and turbo coding for 3GPP LTE systems with limited feedback, in: *Proc. 79th IEEE Veh. Technol. Conf. (VTC 2014 Spring)*, Seoul, Republic of Korea, 2014, pp. 1–5.
- [18] W. Luo, K. Balachandran, S. Nanda, K. Chang, Packet size dependent link adaptation for wireless packet data, in: *Proc. IEEE Global Telecommun. Conf. (GLOBECOM 2000)*, Vol. 1, San Francisco, United States, 2000, pp. 53–56.
- 635 [19] J. Gozávez, M. López-Benítez, O. Lázaro, Link adaptation algorithm for improved wireless transmission of delay-sensitive packet data services, *Electronics Letters* 41 (14) (2005) 813–815.
- [20] C. Kodikara, S. N. Fabri, A. M. Kondoz, Link adaptation for real-time video communications in E-GPRS networks, *IEEE Proc.-Commun.* 151 (5) (2004) 438–444.
- [21] G. Li, S. Jin, F. Zheng, X. Gao, X. Wang, Energy efficient link adaptation for downlink transmission of LTE/LTE-A systems, in: *Proc. IEEE 78th Veh. Technol. Conf. (VTC 2013 Fall)*, Las Vegas, United States, 2013, pp. 1–5.
- 640 [22] E. Eraslan, C.-Y. Wang, B. Daneshrad, Practical energy-aware link adaptation for MIMO-OFDM systems, *IEEE Trans. Wireless Commun.* 13 (1) (2014) 246–258.
- [23] A. J. Goldsmith, S.-G. Chua, Variable-rate variable-power MQAM for fading channels, *IEEE Trans. Commun.* 45 (10) (1997) 1218–1230.
- 645 [24] X. Qiu, K. Chawla, On the performance of adaptive modulation in cellular systems, *IEEE Trans. Commun.* 47 (6) (1999) 884–895.
- [25] K. L. Baum, T. A. Kostas, P. J. Sartori, B. K. Classon, Performance characteristics of cellular systems with different link adaptation strategies, *IEEE Trans. Veh. Technol.* 52 (6) (2003) 1497–1507.
- [26] Y. Zhao, Theoretical study of link adaptation algorithms for adaptive modulation in wireless mobile communication systems, in: *Proc. IEEE Int'l. Conf. Universal Personal Commun. (ICUPC 1998)*, Vol. 1, Florence, Italy, 1998, pp. 587–591.
- 650 [27] R. Sámano-Robles, A. Gameiro, A performance model for maximum ratio combining receivers with adaptive modulation and coding in Rice fading correlated channels, in: *Proc. 19th IEEE Symp. Computers and Commun. (ISCC 2014)*, Funchal, Portugal, 2014, pp. 1–6.
- [28] M. López-Benítez, Throughput performance models for adaptive modulation and coding under fading channels, in: *Proc. IEEE Wireless Commun. and Netw. Conf. (WCNC 2016)*, Doha, Qatar, 2016, pp. 610–615.

- 655 [29] P. H. Tan, Y. Wu, S. Sun, Link adaptation based on adaptive modulation and coding for multiple-antenna OFDM system, *IEEE J. Sel. Areas Commun.* 26 (8) (2008) 1599–1606.
- [30] K. J. Hole, H. Holm, G. E. Øien, Adaptive multidimensional coded modulation over flat fading channels, *IEEE J. Sel. Areas Commun.* 18 (7) (2000) 1153–1158.
- 660 [31] Q. Liu, S. Zhou, G. B. Giannakis, Cross-layer combining of adaptive modulation and coding with truncated ARQ over wireless links, *IEEE Trans. Wireless Commun.* 3 (5) (2004) 1746–1755.
- [32] H. Khodakarami, F. Lahouti, Link adaptation for physical layer security over wireless fading channels, *IET Communications* 6 (3) (2012) 353–362.
- [33] C. Mehlführer, M. Wrulich, J. C. Ikuno, D. Bosanska, M. Rupp, Simulating the long term evolution physical layer, in: *Proc. 17th European Signal Processing Conf. (EUSIPCO 2009)*, Glasgow, United Kingdom, 2009, pp. 1471–1478.
- 665 [34] S. Cui, A. J. Goldsmith, A. Bahai, Energy-constrained modulation optimization, *IEEE Trans. Wireless Commun.* 4 (5) (2005) 2349–2360.
- [35] J. Chuang, X. Qiu, J. Whitehead, Data throughput enhancement in wireless packet systems by improved link adaptation with application to the EDGE system, in: *Proc. IEEE 50th Veh. Technol. Conf. (VTC 1999 Fall)*, Vol. 1, Amsterdam, The Netherlands, 1999, pp. 456–460.
- 670 [36] 3rd Generation Partnership Project, Technical Specification Group Radio Access Network; Evolved Universal Terrestrial Radio Access (E-UTRA); Physical layer procedures (Release 15), Tech. Rep. 3GPP TS 36.213, 3GPP, v15.0.0 (Dec. 2017).
- [37] G. D. Sworo, K. R. Dandekar, M. Kam, Reconfigurable antennas and link adaptation algorithms for MIMO-OFDM wireless systems, *EURASIP J. Wireless Commun. and Netw.* (2015) 1–15.
- [38] P. H. Tan, Y. Wu, S. Sun, Link adaptation based on adaptive modulation and coding for multiple-antenna OFDM system, *IEEE J. Sel. Areas Commun.* 26 (8) (2008) 1599–1606.
- 675 [39] T. L. Jensen, S. Kant, J. Wehinger, B. H. Fleury, Fast link adaptation for MIMO OFDM, *IEEE Trans. Veh. Technol.* 59 (8) (2010) 3766–3778.
- [40] E. Eraslan, B. Daneshrad, Low-complexity link adaptation for energy efficiency maximization in MIMO-OFDM systems, *IEEE Trans. Wireless Commun.* 16 (8) (2017) 5102–5114.
- 680 [41] B. Can, H. Yomo, E. D. Carvalho, Link adaptation and selection method for OFDM based wireless relay networks, *J. Commun. and Netw.* 9 (2) (2007) 118–127.
- [42] G. Pocovi, K. I. Pedersen, P. Mogensen, Joint link adaptation and scheduling for 5G ultra-reliable low-latency communications, *IEEE Access* 6 (2018) 28912–28922.
- [43] O. Narmanlioglu, R. C. Kizilirmak, T. Baykas, M. Uysal, Link adaptation for MIMO OFDM visible light communication systems, *IEEE Access* 5 (2017) 26006–26014.
- 685